

# Membrane separation of liquid-like droplets

Gerald I. Spijksma\*, Nieck E. Benes<sup>1</sup>, Dave H.A. Blank

*Inorganic Materials Science, Faculty of Science & Technology, and Mesa<sup>+</sup> Research Institute,  
University of Twente, P.O. Box 217, 7500 AE Enschede, The Netherlands*

Received in revised form 26 January 2004; accepted 26 January 2004

## Abstract

Liquid (like) droplets may be separated from the continuous phase in which they are dispersed by employing a membrane. Because droplets are deformable, the separation is not simply based on size; droplets may deform sufficiently to enter pores that are much smaller than the droplets themselves. Such a deformation requires a certain critical pressure drop,  $\Delta p_c$ . Assuming the geometry of the droplet is determined by a natural tendency for a minimum surface area,  $\Delta p_c$  can be shown to depend on the surface tension  $\gamma$ , the contact angle  $\theta$ , and the ratio  $a$  of the radii of droplet and pore,  $r_d$  and  $r_p$ , respectively. When 100% retention is required,  $\Delta p_c$  should not be exceeded and, hence, this pressure drop corresponds to the highest attainable (critical) flux  $N_c$ . An almost linear increase is predicted for  $\Delta p_c$  with  $a$ . Despite the monotone increase of  $\Delta p_c$ , the critical flux  $N_c$  shows a maximum at  $a \approx -2/\cos(\theta)$ . Hence, on the basis of  $a$  and  $\theta$  an optimal membrane selection can be made. In the absence of affinity ( $\theta = \pi$ ), the pore radius should be approximately two times larger than the initial droplet radius. When affinity is not negligible, the pore radius required to maintain complete retention increases rapidly, i.e., the maximum critical flux decreases and is observed at larger  $a$ . The largest change in maximum attainable  $N_c$  with the contact angle is observed at  $\theta = 0.75\pi$ .

© 2004 Elsevier B.V. All rights reserved.

**Keywords:** Aspiration; Laplace equation; Droplet deformation; Maximum flux

## 1. Introduction

In the descriptions of separations involving membranes, dynamic deformations of species to be separated are generally neglected. For separations based on differences in, e.g., mass or charge the assumption of invariable species geometry is usually not a critical one. However, for separations based on size, possible deformations of species can be expected to have a significant influence. In those cases, a sufficiently large force may cause species to deform enough to enter the pore and, consequently, a pore-size smaller than the species of interest no longer guarantees complete retention. Examples of deformable species include certain large molecules, organisms, cells, and droplets in emulsions [1–5]. Examples of corresponding membrane applications are plentiful (e.g., [6–8]) and in many of these applications a very high, preferably even complete, retention is required.

Although the influence of species deformation on retention has not received much attention in membrane technology literature, there is abundant literature on a related subject; micro-pipette aspiration of (living) cells [9–11]. Micro-pipette aspiration is considered to be a well-established tool for determining the viscosity and cortical tension of cells [9–11]. In descriptions of micro-pipette aspiration, the focus is on kinetic deformation and recovery behavior of a cell, while transport of the continuous phase is not explicitly explored. Furthermore, affinity of cells for the micro-pipette can be assumed absent. In the following, we present a model for separation of liquid-like droplets, taking into account the affinity of droplets for the membrane material. We will focus our discussion on the maximum pressure allowed to avoid aspiration of a deformable droplet into a capillary and the maximum value of the flux of the continuous phase.

## 2. Problem definition

We will consider the separation of a mixture of two liquids, one of which (denoted by A) is dispersed in the other

\* Corresponding author. Tel.: +31-534892998;  
fax: +31-534894683.

E-mail address: [g.i.spijksma@utwente.nl](mailto:g.i.spijksma@utwente.nl) (G.I. Spijksma).

<sup>1</sup> Current address: Process Development Group, Dept. Chem. Eng., Technical University of Eindhoven, P.O. Box 513, 5600 MB Eindhoven, The Netherlands.

(denoted by B) in the form of droplets with radius  $r_d$ . The volume fraction of the droplets is much smaller than that of the continuous phase and, hence, effects such as cake formation of the deformable droplets [12] can be disregarded. The droplets are to be (completely) retained by a membrane, which is permeable for the continuous phase B. The membrane is assumed to contain cylindrical pores with a distinct pore radius  $r_p$ . Transport of the continuous phase occurs via laminar viscous flow and, hence, is pressure driven. The corresponding expression for the flux of the continuous phase is

$$N = n_{\text{pore}} \frac{r_p^2}{8\eta_B L} \Delta p \quad (1)$$

where we used  $\Delta p \equiv p_{\text{high}} - p_{\text{low}}$ ,  $n_{\text{pore}}$  is the number of pores that are not sealed by a droplet, and  $L$  the membrane thickness. Since the concentration of droplets is assumed to be low, the blocking of pores by droplets will have a negligible effect on the magnitude of the flux of the continuous phase. The objective is to find a maximum value for the flux  $N$ , while the droplets cannot fully enter the pore.

In order to obtain a maximum value for the flux, an expression is required for the pressure drop at which droplets are on the brink of entering the pore; the critical pressure drop  $\Delta p_c$ . This critical pressure drop can be related to the ratio of the radii of droplets and pore

$$a \equiv \frac{r_d}{r_p} \quad (2)$$

Due to the deformability of the droplets they can enter a pore even when  $a > 1$ , provided that a sufficiently large force, i.e., pressure drop, is exerted to give rise to the required change in geometry of the droplet. The extent of such a pressure drop is directly related to the increase in surface area of the droplet. Assuming a natural tendency towards a minimum surface area, the geometry of a deformed droplet will be as depicted in Fig. 1a.

Drury and Dembo [13] performed a numerical simulation study on the hydrodynamics of human neutrophils during micro-pipette aspiration. They showed that for not too large

capillary numbers  $C = \Delta p / \Delta p_c$  the shape of the neutrophils is, at any given instant, indeed close to that corresponding with minimum surface area. In our study, the capillary numbers do not exceed unity. Other assumptions for the droplet shape may be possible. For instance, Park et al. [14] assumed that the deformed shape does not correspond to a minimum surface area. However, their choice does not seem physically realistic, and leads to an expression for  $\Delta p_c$  that diverges when  $a$  is not close unity.

When there is affinity of the droplet for the membrane material, the angle between the droplet surface and membrane material cannot surpass the contact angle, which can be calculated from Young's equation [15]

$$\cos(\theta_{\text{AM}}) = \frac{\gamma_{\text{BM}} - \gamma_{\text{AM}}}{\gamma_{\text{AB}}} \quad (3)$$

In Eq. (3), the subscripts A, B and M refer to the two liquids and the solid material, respectively. Fig. 1b depicts an example of a deformed droplet for which  $\theta < \pi$  ( $180^\circ$ ), tacitly assuming that the shape is again determined by the droplets tendency to achieve a minimum surface area.

### 3. Aspiration

The geometry of a partly aspirated droplet can be visualized as being comprised of two partial spheres, as shown in Fig. 1, one inside and one outside the pore. For each sphere, the curvature of the surface is determined by the pressure difference across the droplet surface, according to the well-known Laplace equation  $r \Delta p = 2\gamma$  [15]. Hence, the equilibrium pressure drop  $\Delta p$  (Pa) over the droplet required to counter the increase in surface area is

$$\Delta p = 2\gamma \left( \frac{1}{r_1} - \frac{1}{r_2} \right) \quad (4)$$

where  $r_2$  and  $r_1$  are the radii (m) as depicted in Fig. 1, and  $\gamma$  the surface tension ( $\text{N m}^{-1}$ ). Due to the conservation of volume of the initial droplet, i.e.,

$$V_0 = V_1 + V_2 \quad (5)$$

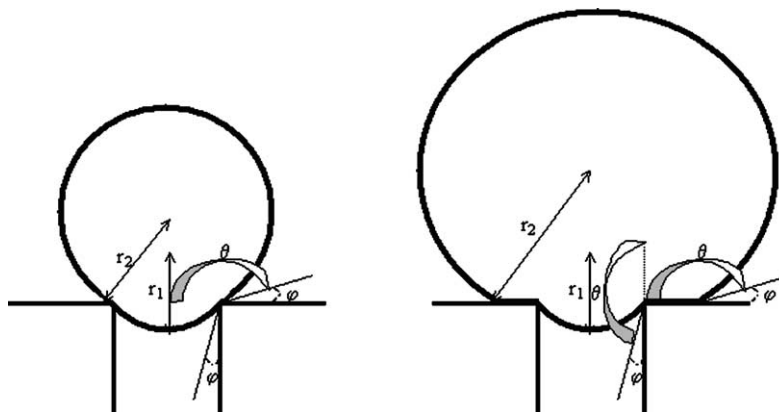


Fig. 1. Schematic representation of the deformation of a partly aspirated droplet when: (a) the contact angle is not exceeded and (b) the contact angle is exceeded.

the values of  $r_1$  and  $r_2$  are interdependent. The initial volume of the droplet is  $V_0 = \frac{4}{3}\pi r_0^3$ . For the volume of the partial droplets inside and outside the pore, the following integral should be solved

$$V_i = \pi \int_{x_0}^{x_E} (r_i^2 - x^2) dx \quad (6)$$

with corresponding integral boundaries;

$$\text{for } V_1 : x_0 = -r_p \tan(\theta), \quad x_E = -r_p/\cos(\theta) \quad (7)$$

$$\begin{aligned} \text{for } V_2 : x_0 &= -r_2, \\ x_E &= \sqrt{r_2^2 - r_p^2}, \text{ (or } x_E = -r_2 \cos(\theta) \\ &\text{when the contact angle is reached)} \end{aligned} \quad (8)$$

For each aspiration depth, the radius  $r_1$  is directly related to  $r_p$  and  $\rho$ , and the value of  $r_2$  follows from the conservation of volume (Eq. (5)). Substitution of  $r_1$  and  $r_2$  in Eq. (4) yields the value for the  $\Delta p$  required to achieve the deformation related to the aspiration depth. In Fig. 2,  $\Delta p$  is plotted as a function of the normalized aspiration depth  $\rho$ , defined as the ratio of the aspiration depth  $z$  over the pore radius  $r_p$ :

$$\rho \equiv \frac{z}{r_p} \quad (9)$$

The behavior of  $\Delta p$  with  $\rho$  is determined by two counteracting phenomena. The equilibrium pressure drop  $\Delta p$  will increase with  $\rho$  due to the decrease in  $r_1$ , while  $\Delta p$  will decrease with  $\rho$  due to the decrease in  $r_2$ . For infinitely large droplets, i.e., infinitely  $a$ , the latter phenomena is absent and a monotone decrease of  $r_1$  with  $\rho$  is observed until the contact angle  $\theta$  is reached at

$$\rho = \frac{\sin(\theta) - 1}{\cos(\theta)} \quad (10)$$

beyond which  $r_1$  no longer changes. From Fig. 2, it can be seen that such a behavior is already observed for, e.g.,  $a = 5$ . For  $\theta = \pi$  (no affinity),  $\Delta p$  increases with  $\rho$  until a maximum value is reached at  $\rho \approx 1$ , beyond which  $\Delta p$  very slowly decreases with further increasing  $\rho$ . For  $\theta = 0.8\pi$ , the maximum value of  $\Delta p$  is reached at  $\rho \approx 0.51$  (the value predicted by Eq. (10)). When  $a = 1.2$ , the decrease in  $r_2$  with  $\rho$  is not negligible and, for  $\theta = \pi$ , the two counteracting phenomena result in a maximum value of  $\Delta p$  at  $\rho = 0.90$ . Further increase of  $\rho$  is now accompanied by an apparent decrease in  $\Delta p$ . The latter maximum  $\Delta p$  is about 5% higher than the value at the  $\rho$  predicted by Eq. (10).

### 3.1. Critical pressure drop

The maximum value of  $\Delta p$  observed in Fig. 2 corresponds to the critical pressure drop  $\Delta p_c$  [16]. When the pressure drop exceeds  $\Delta p_c$  complete aspiration of the droplet into the capillary will occur. Calculation of  $\Delta p_c$  is rather strenuous and for the analysis of micro-pipette aspiration of living cells experiments it is commonly assumed that  $\Delta p_c$  is observed at the value of  $\rho = 1$  (e.g., [11]). Allowing for affinity ( $\theta \leq \pi$ ) the critical aspiration depth obeys Eq. (10). The corresponding critical pressure drop can be calculated from

$$\Delta p_c = -2\gamma \left( \frac{\cos(\theta)}{r_p} + \frac{1}{r_2} \right) \quad (11)$$

When assuming  $r_2 = r_0$ , which is common for micro-pipette aspiration, Eq. (11) simplifies to

$$\frac{r_p \Delta p_c}{2\gamma} = - \left( \cos(\theta) + \frac{1}{a} \right) \quad (12)$$

The actual value of  $r_2$  is calculated from the conservation of volume. It can be shown that the critical pressure drop

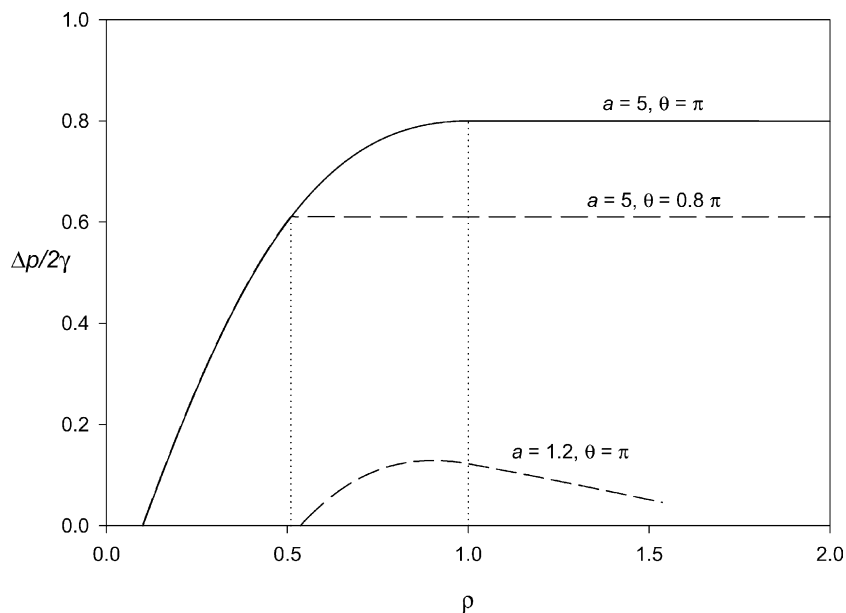


Fig. 2. Equilibrium pressure difference as function of the normalized aspiration depth  $\rho$ . The dashed lines (---) correspond to Eq. (10).

obeys

$$\frac{r_p \Delta p_c}{2\gamma} = \left( -\cos(\theta) - \frac{1}{f(a, \theta)} \right) \quad (13)$$

The form of expression  $f(a, \theta)$  depends on whether the angle between the outer droplet and the surface ( $\theta$  in Fig. 1b) has reached the contact angle. An elegant solution for Eq. (13) was presented by Nazzal and Wiesner [17],

$$f(a, \theta) = \frac{1}{\cos(\theta)} \times \left( \frac{2 - 3 \cos(\theta) + \cos^3(\theta)}{-4a^3 \cos^3(\theta) - 2 + 3 \sin(\theta) - \sin^3(\theta)} \right)^{-1/3} \quad (14)$$

who assumed that the angle between the outer droplet and the membrane always equals  $\theta$ . Obviously, for small  $a$  and large  $\theta$  values this assumption is physically not plausible.

In Fig. 3,  $r_p \Delta p_c / 2\gamma$  is plotted as a function of  $a$ , for various  $\theta$ . The squares correspond to simulations in which complete aspiration is assumed to occur when the maximum value of  $\Delta p$  is observed (as in Fig. 2). For the lines, triangles and dots the critical aspiration depth is calculated from Eq. (10). The continuous lines are solutions to Eq. (13), while the dots correspond to the approximate solutions from Eq. (12) and the triangles to the expression of Nazzal and Wiesner (Eq. (14)). From the figure it is clear that the deviations between the different solutions are negligible for larger  $a$  and only small deviations are observed for small  $a$ . All solutions based on Eq. (10) deviate less than 5% (for  $a = 1.2$ ) compared to the accurate solution, obtained using Eq. (13).

The behavior of  $r_p \Delta p_c / 2\gamma$  with  $a$  can be explained as follows. For  $\theta = \pi$  and  $a = 1$  the droplet just fits into the pore and the critical pressure,  $\Delta p_c$ , is 0. If the droplet is slightly

larger than the pore, a larger value for the pressure difference is required to push it into the pore, i.e.,  $\Delta p_c$  increases with  $a$ . When the droplet radius is large compared to that of the pore, the influence of  $r_2$  becomes negligible. Eq. (11) reduces to the standard Laplace equation and an asymptotic value is observed for  $r_p \Delta p_c / 2\gamma$ . For  $1/2\pi < \theta < \pi$ , Eq. (12) predicts that the  $\Delta p_c$  is zero at  $a_0 \approx -1/\cos(\theta)$ , thus  $a$  should always be larger than  $a_0$ . This is due to the enhanced affinity of the droplets for the membrane material. Even when the droplet radius is slightly larger than that of the pore, the affinity causes the droplet to be aspirated, unless a negative pressure drop is exerted. These negative values correspond to negative values of the flux and are here for of no interest in this study. The increase of  $\Delta p_c$  with  $a$  is less when the affinity increases (i.e.,  $-\cos(\theta)$  closer to zero), which is expected since the enhanced affinity will make it easier for the droplets to enter the pore.

### 3.2. Flux

Although  $\Delta p_c$  always increases with  $a$ , the behavior of the flux of the continuous phase  $N$  is less straightforward, given that it is proportional to the critical pressure multiplied with  $r_p^2$

$$N \sim r_p^2 \Delta p_c \quad (15)$$

From Fig. 3, the dependency of the flux on  $a$  can easily be predicted. For  $a \leq a_0$ , the flux,  $N$ , is zero because no pressure drop can be exerted. When  $a$  is slightly increased, a pressure drop can be applied on the droplet without pushing it into the pore and thus an increase in the flux is expected. For a large value of  $a$ ,  $r_p \Delta p_c$  reaches an asymptotic value of  $-\cos(\theta)$ . The value of the flux is equal to the product of the pore

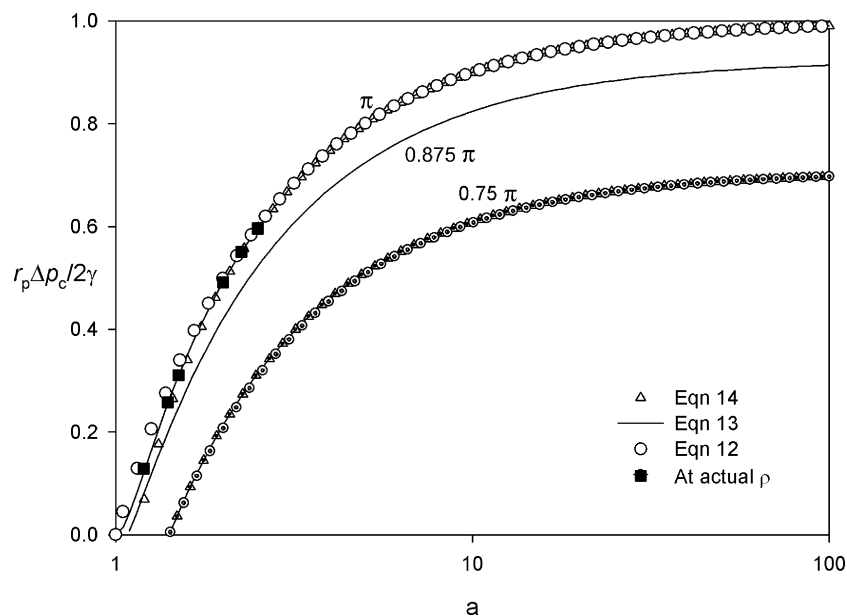


Fig. 3. The line represent the left hand side of Eq. (13) as a function of  $a$ , for various  $\theta$ . The dots and triangles are the results using, respectively, Eqs. (12) and (14). The squares correspond to calculations without employing the approximating Eq. (10), i.e., using the actual critical aspiration depths.

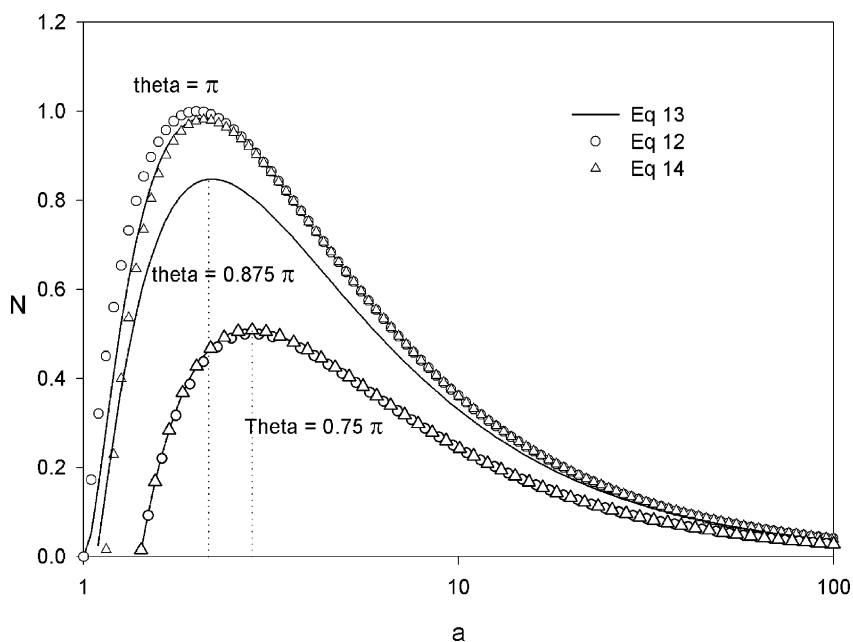


Fig. 4. Trend of the flux versus  $a$  calculated for various  $\theta$ . Continuous line: solution to Eq. (13); triangles: expression of Nazzari and Wiesner; dots: Eq. (12). Y-axis scaled with respect to  $4/r_0$ , so that the  $N_c(\text{max})$  predicted by Eq. (11) equals unity for  $\theta=\pi$ .

radius and this asymptotic value and, hence, a decrease of the flux with  $a$  is expected. The initial increase and subsequent decrease of the flux with  $a$  requires a maximum in its value. The value of  $a$  at which this maximum is observed ( $a_{\text{max}}$ ) can be approximated by substitution of Eq. (12) in Eq. (15) and subsequent differentiation

$$a_{\text{max}} \approx \frac{-2}{\cos(\theta)} \quad (16)$$

The corresponding maximum (or optimal) value of  $N_c$  is proportional to

$$N_c(\text{max}) \sim \left( r_p^2 \frac{\Delta p_c}{2\gamma} \right)_c = \frac{r_0 \cos^2(\theta)}{4} \quad (17)$$

In Fig. 4, the shape of  $N_c$  versus  $a$  is depicted, as predicted from the various solutions for  $\Delta p_c$  discussed in this paper. The different solutions are in agreement, where only for small  $a$  deviations are visible in the graph. From the figure it is clear that indeed at a particular  $a_{\text{max}}$  a maximum is observed for  $N$ . For  $\theta = \pi$ , the figure shows a maximum in the value of the flux when the droplets are approximately 2.07 times larger than the pore (Eq. (16) predicts a value of 2). This would be the optimal choice for our objective; a maximum value for the flux of the continuous phase, combined with complete retention of the droplets.

The decrease of  $r_p^2 \Delta p_c$  in the case of enhanced affinity is clearly visible in the figure. The zero value of the flux requires droplets that are larger than the pores. The maximum value of the flux is observed at a larger ratio of the droplet and pore sizes, as predicted by  $a_{\text{max}} \approx -2/\cos(\theta)$ . The value of maximum flux reduces with increase in affinity, especially for contact angles  $\theta$  close to  $0.75\pi$  (since  $(\partial N_c(\text{max})/\partial \theta) \sim \sin \theta \cos \theta$ ).

While for contact angles close to  $\pi$ , the maximum critical flux is only slightly influenced by a change in  $\theta$ .

#### 4. Conclusions

When a critical pressure drop  $\Delta p_c$  is exceeded, liquid-like droplets will enter a capillary. The value of  $\Delta p_c$  depends on the surface tension, the affinity of the droplet for the capillary, and the ratio  $a$  of the radii of the initial droplet and capillary. An almost linear increase is observed for  $\Delta p_c$  with  $a$ . The product  $r_p \Delta p_c$  increases with  $a$  until a stationary value ( $\approx -\cos(\theta)$ ) is reached. The flux of the continuous phase, corresponding to  $\Delta p_c$ , shows a maximum at  $a_{\text{max}} \approx -2/\cos(\theta)$ . The highest value of this optimal flux, and the corresponding lowest value of  $a_{\text{max}}$  ( $\sim 2.07$ ), are observed when affinity of the droplets for the membrane material is negligible ( $\theta = \pi$ ). When affinity is not negligible a smaller pore is required to retain the droplets ( $a_{\text{max}}$  increases) and the value of the optimal flux decreases accordingly. The largest sensitivity of the optimal flux with changing  $\theta$  is observed at  $\theta = 0.75\pi$ , while for  $\theta = \pi$  the change in optimal flux is small with changing contact angle.

#### References

- [1] S.S. Madaeni, A.G. Fane, G.S. Grohmann, J. Membr. Sci. 102 (1995) 65.
- [2] T. Urabe, K. Yamamoto, S. Ohgaki, J. Membr. Sci. 115 (1996) 21.
- [3] S.S. Madaeni, Water Res. 33 (1999) 301.
- [4] S. Geiger, N. Jager-Lezer, S. Tokgoz, M. Seiller, J.-L. Grossiord, J. Colloid Surf. A 157 (1999) 325.

- [5] E.M. van Voorthuizen, H.J. Ashbolt, A.I. Schafer, *J. Membr. Sci.* 194 (2001) 69.
- [6] T. Tetsuzo, M. Mineshima, *J. Membr. Sci.* 44 (1989) 47.
- [7] P.S. Malchesky, T. Horiuchi, J.J. Lewandowski, Y. Nosè, *J. Membr. Sci.* 44 (1989) 55.
- [8] A. Yeung, E. Evans, *Biophys. J.* 56 (1989) 139.
- [9] N.P. Perepechkina, L.P. Perepechkin, *J. Membr. Sci.* 160 (1999) 1.
- [10] E. Evans, A. Yeung, *Biophys. J.* 56 (1989) 151.
- [11] R.M. Hochmuth, *J. Biomech.* 33 (2000) 15.
- [12] W.M. Lu, K.-L. Tung, C.-H. Pan, k.-J. Hwang, *J. Membr. Sci.* 198 (2002) 225.
- [13] J.L. Drury, M. Dembo, *Biophys. J.* 76 (1999) 110.
- [14] S.-H. Park, T. Yamaguchi, S.-I. Nakao, *Chem. Eng. Sci.* 56 (2001) 3539.
- [15] P.W. Atkins, *Physical Chemistry*, fifth ed., Oxford University Press, Oxford, 1994.
- [16] J. Derganc, B. Bozic, S. Svetina, B. Zeks, *Biophys. J.* 79 (2000) 153.
- [17] F.F. Nazzal, M.R. Wiesner, *Water Environ. Res.* 68 (1996) 1187.